22nd International Symposium on Plasma Chemistry
July 5-10, 2015; Antwerp, Belgium

An investigation of a low-pressure DC glow discharge on Ni nanoparticle-decorated cathodes

M.D.G. Evans[1], M.A. McArthur[1] and S. Coulombe

[1] *Authors contributed equally to the work presented*
Plasma Processing Laboratory, Dept. of Chemical Engineering, McGill University, Montréal, Québec, Canada

Abstract: A study of Ni nanoparticles-decorated cathodes was performed to evaluate their performance in a low-pressure DC glow discharge configuration. Optical emission spectroscopy was performed to evaluate changes in the glow discharge when various Ni nanoparticles-decorated stainless steel and carbon nanotube-covered stainless steel cathodes were used. The addition of Ni nanoparticles decreased the breakdown voltage required and increased the electron temperature in the negative glow region.

Keywords: low-pressure DC glow discharge, cathodes, Ni nanoparticles, multi-walled carbon nanotubes, optical emission spectroscopy

1. Introduction

Low-pressure DC glow discharges have been studied extensively over the last century. From the initial identification of charged particles by Thomson in 1897 [1], DC glow discharges have been well recognized in scientific advancement. However, much can still be learned from these relatively simple systems. For example, the effect of the chosen cathode material can be examined to determine cathode-dependent properties of the subsequent glow.

From the beginning, electrode erosion as a result of the interaction with the electrical discharge has been a concern. The most recent works in our laboratory aim at introducing nanostructures to locally enhance the electric field strength [2], thus favouring electron emission, but also to add chemically-tuneable functional groups onto the electrode surface to favour a synergetic interaction with the discharge [3]. Novel materials that show promise are carbon nanotubes (CNTs), as they can be grown rather easily on stainless steel, are easy to functionalize, and form an open, large-surface area network. Looking back, one realizes that the interest in CNT-based electrodes have been identified almost immediately after the discovery of CNTs [2] as potential candidates for plasma-based applications, owing to their unique (electrical, mechanical, and thermal) properties and geometry. Initial studies on CNT degradation in oxygen glow discharges may provide insight towards the use of these materials as electrodes in emission applications, such as fluorescent lighting or flat panel displays [4]. An additional benefit to these electrodes is the ability to function in alternative source gases that produces UV-radiation, such as water vapour, thus eliminating the use of Hg-containing materials. However, the use of water vapour has its own set of challenges. For example, an incompatible electrode will decompose relatively quickly in the presence of water vapour in a glow discharge.

Over the past decade, our laboratory has developed techniques to produce electrodes consisting of CNT-covered stainless steel (SS/CNT) with/without grafting of oxygen-containing functional groups enhancing the hydrophilicity of the electrodes. These functional groups may offer improved compatibility with a DC glow discharge containing water vapour. Moreover, by using pulsed laser ablation (PLA), CNT-covered SS cathodes can be *decorated* with nanoparticles (NPs) of a conductive material, such as Ni, which may further affect electron emission from these nanometric asperities and certain plasma parameters such as the population of emitting states and gas breakdown voltage.

In this study, we investigate the effects of Ni NPs decoration, grown CNTs, or both on SS cathodes on basic low-pressure DC glow discharge characteristics, namely the ignition and sustaining voltages and electron temperature in the negative glow.

2. Experimental Methodology

2.1 Cathode Preparation

CNT-covered SS cathodes were prepared following the synthesis technique reported in [5]–[7]. Briefly, CNTs were grown by thermal-chemical vapour deposition (t-CVD) directly from commercially available grade 316 stainless steel mesh discs (1.27 cm dia., 400 series; McMaster-Carr, USA) degreased ultrasonically in acetone for 30 min. After 30 min of heating the SS discs at 700 ºC in a tube furnace under continuously flowing Ar (592 ± 5 cm^3 min^{-1}), the carbon source, acetylene, was injected for 4 min at 68 ± 5 cm^3 min^{-1}. The furnace was allowed to cool to room temperature after C_2H_2 injection and the SS/CNT cathodes were removed. The average mass density of the CNTs was 0.135 mg cm^{-2}. These cathodes were used as a basis for further modification by plasma functionalization (f-SS/CNT cathodes) and decoration by Ni NPs (f-d-SS/CNT cathodes).

Plasma functionalization ("f-" identifier) of the SS/CNT cathodes was done to graft hydrophilic oxygen containing surface groups, e.g. hydroxyls, carboxyls, and carbonyls [8], to the CNT walls. Functionalization was done by exposing the cathodes to a low-pressure (1.25 Torr) capacitively-coupled radio-frequency (RF) glow discharge. An $Ar/O_2/C_2H_6$:250/5/1 cm^3 min^{-1} gas mixture was metered by mass flow controllers (MFC, Brooks 5050E; Brooks, USA). The RF glow discharge was sustained at 20 W for 5 min using a continuous wave 13.56 MHz power supply (Advanced Energy Cesar; Advanced Energy, USA).

Decoration of the cathodes ("d-" identifier) was done in a custom-designed PLA system with a base pressure of ~2.5 mTorr. A frequency-tripled ns pulsed Nd:YAG laser (355 nm, 10 Hz, 5 ns pulse duration; Brilliant B10, Quantel, France) was focused onto a Ni target (2.54 cm dia., 0.32 cm thickness, 99.9%, Kurt J. Lesker Co., USA) at a 45° angle for 40 min. From previous optimization experiments [6], these conditions showed uniform NP dispersion along the exposed sample with a very narrow size distribution (~4 nm dia.).

2.2 Apparatus and Measurement Techniques

Fig. 1 shows a schematic of the geometry and apparatus used to perform the glow discharge experiments on the modified SS cathodes. The left side of Fig. 1 details the optical emission spectroscopy (OES) setup used whereas the right side displays the DC circuit used to ignite the glow. Details on the insulated cathode holder, DC glow discharge chamber, and vacuum handling systems can be found in [4], [9]. The base pressure of the chamber reached ~16 mTorr using a two-stage roughing pump. The flow of Ar was maintained at 312 ± 5 cm^3 min^{-1} by MFC (Brooks 5050E; Brooks, USA) which allowed for a chamber pressure P = 1 Torr. The inter-electrode distance was set at d = 1 cm for all experiments (Pd = 1 Torr.cm).

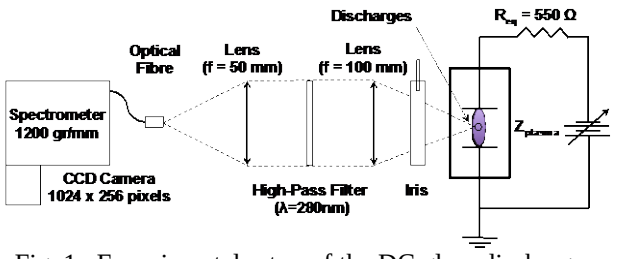

Fig. 1. Experimental setup of the DC glow discharge.

OES was performed in a similar fashion as described in [10]. Briefly, the light emitted from the glow discharge passes through an MDC-compatible quartz window and into a system of optical elements consisting of an iris, a lens (focal length = 50 mm), a high-pass filter (λ > 280 nm), and another lens (focal length = 100 mm) before entering an optical fibre attached to the spectrometer (Acton 2300i, Princeton Instruments, USA) equipped with a CCD camera (PIXIS 256, Princeton Instruments, USA) in the geometry displayed in Fig. 1. The exposure time of the CCD was 100 ms, and 100 accumulations of the signal were used to produce the recorded spectra.

3. Results and Discussion

3.1 Cathode Characterization

Figs. 2a-d show scanning electron micrographs (SEMs) of (a) bare SS mesh, and SS/CNT at (b) 1000X, (c) 2000X and (d) 10000X magnification prior to operation as DC glow discharge cathodes. In general, the CNTs are ~60-100 nm in dia. and are ~1-8 μm in length. The CNTs form a relatively open 3-D matrix, which can readily accept functionalization.

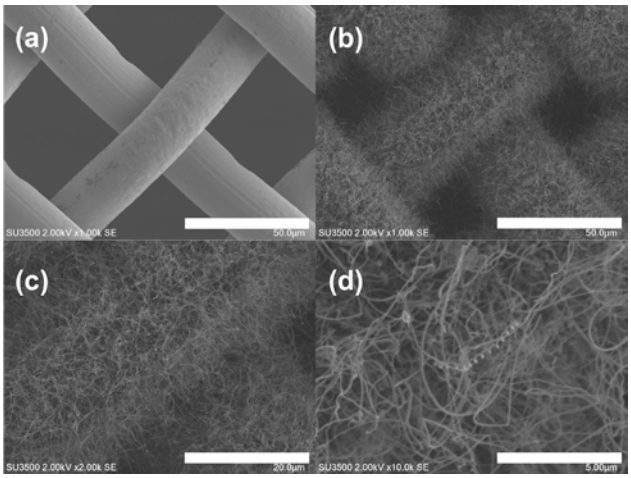

Fig. 2. SEMs of (a) 316 SS mesh, SS/CNT at magnification of (b) 1000X, (c) and (d) 10000X prior to exposure to the DC glow discharge.

3.2 DC Breakdown Experiments

Fig. 3 shows the values of the required ignition voltage of the DC glow discharge for all the prepared cathode materials as well as a characteristic image of the glow (inset; cathode on the right side). In order to obtain the breakdown voltage threshold, the voltage was progressively increased at a fixed pressure and inter-electrode gap until the formation of a plasma channel took place. The breakdown experiment was repeated 30 times for each sample in order to ensure reproducibility of the experiment.

The observed breakdown voltage with the bare SS mesh is 275 V at Pd = 1 Torr.cm, which is close to the typical minimum value of the Paschen curve for a flat surface [11]. With CNTs grown on the SS (SS/CNT), this breakdown voltage increases to 309 V. Since the CNTs are not grown with vertical alignment, it is postulated that the electron emission of the electrode decreases with the growth of carbon nanostructures on the SS mesh consequently increasing the required voltage to produce gas breakdown. The presence of grafted carboxylic functional groups on the CNT surface does not seem to influence the breakdown voltage significantly. The addition of Ni nanoparticles on the cathodes, on the other hand, leads to a modest, yet observable, decrease of the

breakdown voltage; a 6 V reduction for the d-SS with respect to the bare SS cathode, and a 4 V reduction for the d-f-SS/CNT with respect to the f-SS/CNT cathode. Although the conductivity of the Ni NPs is superior to that of the CNTs and SS mesh, the reduction of the breakdown voltage cannot be attributed to this. Cu mesh electrodes, which have a higher electrical conductivity than Ni, showed higher breakdown voltage values (~287 V) when tested on the experimental setup (data not shown here). The addition of NPs onto the surface most likely adds localized regions on which the electric field strength is enhanced, thus favouring electron emission.

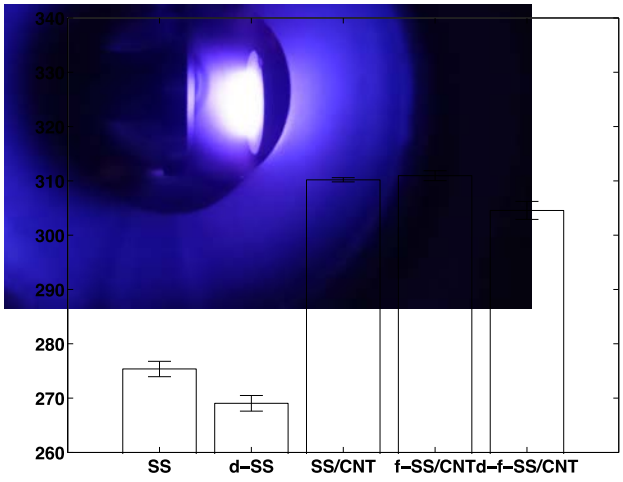

Fig. 3. Ignition voltage in Ar for the various cathodes at Pd = 1 Torr.cm. Inset shows a picture of the discharge, with the bright negative glow.

3.3 Plasma Characterization

To the naked eye, only the negative glow and Faraday dark space can be observed in the current arrangement and operating conditions. Fig. 4 shows a typical OES spectrum obtained over the near-UV to near-IR range with the optical setup focused on the negative glow. The inset to Fig. 4 displays an expanded view of the low-wavelength region (λ < 370 nm). Emission from the OH ($A^2\Sigma$ - $X^2\Pi$) and N_2 ($C^3\Pi_u$ –$B^3\Pi_g$) systems are observed along with the predominant emission of the Ar I lines in the near-IR region. Air-related species are observed in the plasma emission spectrum due to trace contaminants in the system's input.

Fig. 5 shows the absolute intensities of the Ar I $2p_4$-$1s_3$ line for (a) bare SS and d-SS cathodes and (b) SS/CNT, f-SS/CNT, and d-f-SS/CNT cathodes. At an applied DC voltage of 350 V, the Ar, N_2, and OH atomic and molecular system emissions are increased by factors of 5.50, 3.48 and 4.07, respectively with the addition of Ni NPs on bare SS mesh. An increase by factors of 2.01, 1.83 and 1.46, respectively, for the same emission systems was observed on d-f-SS/CNT cathode when compared to the SS/CNT cathode.

To explain the changes in the appearance and relative intensity of the $2p_4$-$1s_3$ transition (λ = 728 nm), the convolution of Eq. 1 with the instrumental slit function was used to model the relative intensities of the Ar I peaks.

$$I(\lambda) = \frac{n_{tot} A_{(e',e'')} g_{e'} \exp\left(-\frac{E_{e'}}{kT_e}\right)}{\sum_{e'} g_{e'} \exp\left(-\frac{E_{e'}}{kT_e}\right)} \frac{hc}{\lambda} \qquad (1)$$

The ratio of each selected transition to the $2p_9 \rightarrow 1s_5$ line (λ = 812 nm) is fitted using the above model to find the corresponding electron temperature. Fig. 5 shows the emission intensity of the Ar I $2p_2 \rightarrow 1s_4$ transition normalized to the $2p_9 \rightarrow 1s_5$ line, and for which an electron temperature is calculated for all cathodes tested in this study (350 V, Ar, P = 1 Torr, d = 1 cm).

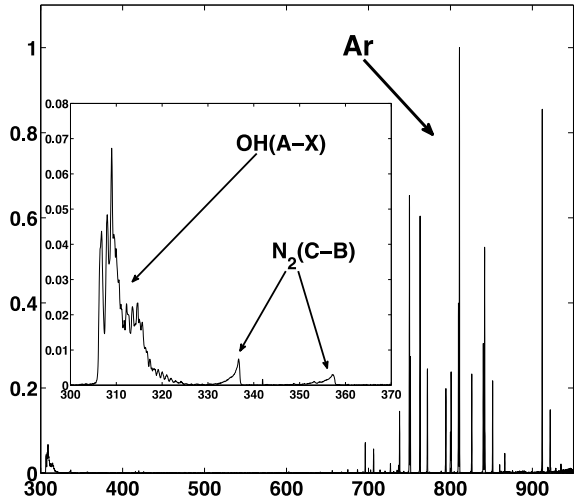

Fig. 4. Typical OES spectrum of the DC glow discharge indicating species of interest. Inset displays wavelengths below 370 nm.

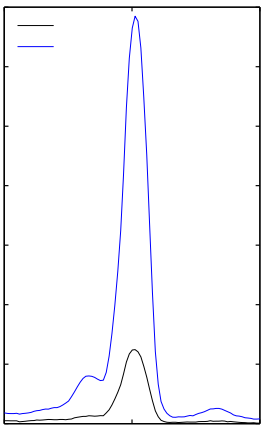

Fig. 5. Absolute intensities of the $2p_4$-$1s_3$ transition for the (a) SS and d-SS and (b) SS/CNT, f-SS/CNT and d-f-SS/CNT cathodes.

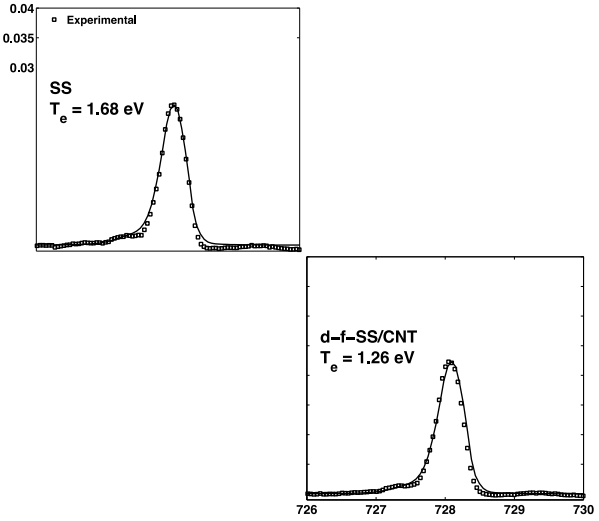

Fig. 6. Experimental and modelled emission line profile for the Ar I $2p_4$-$1s_3$ transition for all the cathodes.

Fig. 6 shows the modelled and experimentally obtained (negative glow) Ar I $2p_4$-$1s_3$ emission line for the various cathode materials. The results show that the electron temperature increases in the negative glow when Ni NPs are present on the stainless steel mesh. The addition of Ni NPs appears to further populate the $2p_4$ state and several other states of the Ar atom for an identical sustaining voltage. The exact reason for this significant increase of the electron temperature with the addition of seemingly insignificant mass of Ni NPs is still uncertain. The role played by the Ni NPs at the cathode's surface remains to be investigated, but it can potentially be linked to the electron emission and consequently, to the self-sustaining conditions.

4. Conclusions

Ni NPs dispersed on a SS mesh cathode appear to decrease the ignition voltage of a low-pressure DC glow discharge in Ar. Additionally, the presence of Ni NPs results in a significantly larger electron temperature in the negative glow region. The absolute intensity of the OH, N_2, and Ar species emission increased for the same source voltage. It was also found that non-directionally grown CNTs do not provide a decrease in the breakdown voltage. In fact, the reverse behaviour is observed. It is believed that the non-directional growth of CNTs on SS mesh decreases the emission of electrons at the cathode's surface thus driving the value of the breakdown voltage to increase. Ni NPs-decorated cathodes provide a change in electron temperature and absolute emission intensities of a produced plasma for minimal added mass of Ni and show promise in the field of plasma generation.

5. Acknowledgements

M.A.M. acknowledges the funding support from McGill University through the McGill Engineering Doctoral Award and NSERC through the CGSD award. M.D.G.E. acknowledges the funding support from McGill University through the McGill Engineering Doctoral Award and FRQNT through the B2 award.

6. References

[1] J. J. Thomson, Philosophical Magazine, **90**, 25 (2010).

[2] M. Dionne, S. Coulombe, and J.-L. Meunier, "Plasma-enhanced electron emission from carbon nanotube arrays for sustained atmospheric discharges," presented at the ISPC-19, Bochum, Germany, 2009.

[3] L. Vandsburger, S. Coulombe, and J.-L. Meunier, Plasma Processes and Polymers, **11**, 222 (2014).

[4] L. Vandsburger, S. Coulombe, and J. L. Meunier, Carbon, **57**, 248 (2013).

[5] N. Hordy, N.-Y. Mendoza-Gonzalez, S. Coulombe, and J.-L. Meunier, Carbon, **63**, 348 (2013).

[6] M. A. McArthur, L. Jorge, S. Coulombe, and S. Omanovic, Journal of Power Sources, **266**, 365 (2014).

[7] M. A. McArthur, N. Hordy, S. Coulombe, and S. Omanovic, Electrochimica Acta, *in press* (2014).

[8] N. Hordy, J.-L. Meunier, and S. Coulombe, Plasma Processes and Polymers, *in press* (2014).

[9] M. D. Lennox, "Synthesis of zine/zinc oxide nanoparticle-carbon nanotube composites," Ph.D., McGill University, Montreal, Quebec, Canada, 2013.

[10] M. D. G. Evans, F. P. Sainct, F. Aristizabal, J. M. Bergthorson, and S. Coulombe, "Development of a nanosecond pulsed HV atmospheric pressure source: preliminary assessment of its electrical characteristics and degree of thermal nonequilibrium," *to appear* (2015).

[11] O. F. Farag, M. M. Mansour, N. M. El-Sayed, and M. H. Elghazaly, Advances in Applied Science Research, **4**, 146 (2013).